Crystal Structure of ITQ-26, a 3D Framework with Extra-Large Pores

Douglas L. Dorset,*,† Karl G. Strohmaier,† Chris E. Kliewer,† Avelino Corma,‡ Mariá J. Díaz-Cabañas,‡ Fernando Rey,‡ and Christopher J. Gilmore§

Corporate Strategic Research, ExxonMobil Research and Engineering Company, 1545 Route 22 East, Annandale, New Jersey 08801, Instituto de Technología Química, University Politécnica de Valencia, Valencia, Spain, and Chemistry Department, University of Glasgow, Glasgow G12 8QQ Scotland, United Kingdom

Received April 24, 2008. Revised Manuscript Received May 30, 2008

ITQ-26 was synthesized via the fluoride procedure using 1,3-bis-(triethylphosphoniummethyl)-benzene as the structure-directing agent. The unit cell and space group were initially determined from electron diffraction experiments on individual tilted microcrystals, using material that had been sectioned by ultramicrotomy. The material crystallizes in space group *I4/mmm*, where after refining against synchrotron powder data ($\lambda = 0.8714$ Å), $a = 26.7769(8)$ and $c = 13.2505(5)$ Å. Integrated electron diffraction intensities ($hk0 + 0kl$) were assigned phases with the program MICE to yield electrostatic potential maps with the first informative view of the microporous framework. As a constraint for subsequent phasing trials of the powder data with FOCUS, one useful solution was found after 500 000 trials, conforming to the electron crystallographic determination. The final model, refined by Rietveld methods, comprises 7 unique T-sites forming a framework with a straight 12-MR channel along [001]. Two other 12-MR channels are tilted with respect to this one. The T-site density is 14.3 T/1000 A^3.

Introduction

The synthesis of microporous materials aims to assemble atoms into porous space that would support sorbed molecules for catalytic conversions and separation processes. When the size of the sorbed molecule is close to the size of the zeolite cavity, van der Waals and Coulombic forces become important and explain, in part, the high reactivity of zeolites.[1] Various organic structure-directing agents (SDA) have been tested with the aim of controlling the pore shape and size as the inverse of the three-dimensional molecular template topology. Although a direct analogy between template and resultant channel space cannot always be demonstrated, there is ample evidence that the SDA does have an influence on defining the channel geometry.[2] Although SDAs have traditionally been amines and tetraalkylammonium cations, in a few cases, macrocyclic ethers[3] and organometallic cations[4] have also been used. We have recently demonstrated the usefulness of tetraalkylphosphonium cations as structure-directing agents with the discovery of the 12-ring zeolite, ITQ-27, having the IWV framework type,[5] using dimethyldiphenyl phosphonium as the structure-directing agent.

In the search for intersecting large-pore zeolites to process large hydrocarbon molecules, three major approaches have been used for their exploratory synthesis. One has been to employ fluoride ions instead of hydroxide to mineralize the silicate species and stabilize the formation of small cages;[6] the second is the use of very low water containing gels to induce the formation of low framework density zeolites; and the third has been to insert unusual heteroatoms into the T-site framework,[7] such as Zn or Ge. The former approach has the advantage that fluoride partially functions as a templating agent. The latter is beneficial because resultant smaller Ge−O−Ge bond angles stabilize the formation of the D4R often associated with these materials. Computational studies reveal that germanium contents of 2−3 atoms per D4R are most favorable.[8]

This paper describes the crystal-structure determination of ITQ-26, a three-dimensional large-pore germanosilicate zeolite synthesized via the fluoride procedure using 1,3-bis-(triethylphosphoniummethyl)-benzene as the SDA. This study also illustrates useful procedures for solving unknown zeolite structures when powder data are only marginally sufficient to provide an unequivocal structural model. Specifically, the successful application of electron crystallography to an unknown is demonstrated to provide independent structural information to guide the powder determination to a successful outcome.

* Corresponding author. E-mail: d.l.dorset@exxonmobil.com.
† ExxonMobil Research and Engineering Company.
‡ University Politécnica de Valencia.
§ University of Glasgow.

(1) Zicovich, C. M.; Corma, A.; Viruela, P. J. *Phys. Chem.* **1994**, *98*, 10863.
(2) Szostak, R. S., *Molecular Sieves*, 2nd ed.; Blackie Academic & Professional: London, 1998.
(3) Delprato, F.; Delmotte, L.; Guth, J. L.; Huve, L. *Zeolites* **1990**, *10*, 546.
(4) Lobo, R. F.; Tsapatsis, M.; Freyhardt, C. C.; Khodabandeh, S.; Wagner, P.; Chen, C. Y.; Balkus, K. J.; Zones, S. I.; Davis, M. E. *J. Am. Chem. Soc.* **1997**, *119*, 8474.
(5) Dorset, D. L.; Kennedy, G. J.; Strohmaier, K. G.; Diaz-Cabanas, M. J.; Rey, F.; Corma, A. *J. Am. Chem. Soc.* **2006**, *128*, 8862.
(6) Camblor, M. A.; Villaescusa, L. A.; Díaz-Cabañas, M. J. *Top. Catal.* **1999**, *9*, 59.
(7) Corma, A.; Davis, M. E. *Chem. Phys. Chem.* **2004**, *5*, 304.
(8) Sastre, G.; Vidal-Koya, J. A.; Blasco, T.; Rius, J.; Jorda, J. L.; Navarro, M. T.; Rey, F.; Corma, A. *Angew. Chem., Int. Ed.* **2002**, *41*, 4722.

10.1021/cm801126t CCC: $40.75
Published on Web 07/11/2008

Materials and Methods

Zeolite. The germanosilicate was synthesized[9] using 1,3-bis-(triethylphosphoniummethyl)-benzene dihydroxide (*m*-Bz$(Et_3P)_2$-$(OH)_2$) as a structure directing agent in a fluoride medium. A gel was prepared by dissolving 0.62 g of GeO_2 in 24.2 g of 0.31 M solution of *m*-Bz$(Et_3P)_2(OH)_2$ and then adding 5.02 g of tetraethylorthosilicate with stirring until it hydrolyzed. The resulting gel was evaporated in air until all of the ethanol was eliminated and H_2O:SiO_2 < 5. A solution of 48 wt % HF and water was added to reach the final stoichiometry of 0.5 HF:0.25 *m*-Bz$(Et_3P)_2(OH)_2$:0.20 GeO_2:0.80 SiO_2:7.5 H_2O. The zeolite was crystallized in a Teflon-lined autoclave at 175 °C for 6 d under stirring. As shown below, ITQ-17 (BEC) is observed as a contaminant in this material. Chemical analyses indicated that the SDA molecule is intact within the zeolite channels. The recovered zeolite was calcined in air for 3 day at 580 °C.

Sorption. The porosity of the calcined material was measured by absorbing nitrogen and argon, which gave a BET surface area of 257 m^2/g, a micropore volume of 0.12 cm^3/g, and a pore diameter of 7.1 Å.

Synchrotron Powder Diffraction. Debye−Scherrer synchrotron powder diffraction measurements on calcined ITQ-26 in capillaries ($\lambda = 0.87143$ Å) were made at the ExxonMobil beamline X10B at the Brookhaven National Laboratory. (Previously, powder X-ray patterned were obtained on a laboratory instrument with Cu Kα radiation.) In addition to single-crystal electron diffraction evaluations (see below), patterns were also indexed with the Jade software package from MDI, Inc. The crystal structure was eventually solved using the software package FOCUS.[10] Rietveld refinements of the structural models were made with GSAS.[11] Silicate models used for Rietveld refinement were first refined by DLS[12] to optimize bonding parameters.

Electron Diffraction. Transmission electron diffraction measurements were carried out at 300 kV with a FEI/Philips CM-30 instrument. The zeolite sample was first crushed to a fine powder in a mortar and pestle and then suspended in acetone in an ultrasonic bath. Drops of the fine particle suspension were then dried on carbon-film-covered 300-mesh copper electron microscope grids. Later, when the crystallites were observed to be somewhat too thick for electron diffraction observation, microcrystalline preparations were suspended in L. R. White resin and then sectioned with a Reichert Jung Ultracut E-2 ultramicrotome. The sections were cut with a diamond knife and floated onto a water surface to be picked up with 200-mesh Cu grids covered with a holey carbon film.

Selected area electron diffraction patterns were recorded on Kodak SO-163 electron microscope film developed in Kodak HRP developer. Reciprocal spacings in diffraction patterns were calibrated against a gold powder standard.

Upon obtaining useful electron diffraction patterns (e.g., *hk*0 and 0*kl*), resultant films were digitized on a flat-bed scanner and these records were analyzed with the program ELD[13,14] in the computer package CRISP[15] to extract intensities of the individual diffraction spots. No Lorentz correction was applied to these data. Attempts at direct structure analysis with these electron diffraction intensities were made using maximum entropy and likelihood via the computer program MICE.[16] Later, additional trials were made with a new version of MICE[17] modified so that initial solutions identified by a maximum likelihood figure of merit could be screened further by correlation coefficients evaluating matches to the theoretical density histogram for a zeolite,[18] redefined for the electron diffraction scattering factors.

Results

After calcination and dehydration of the sample, the synchrotron powder diffraction pattern from ITQ-26 (Figure 1), although collected to $2\theta = 52°$, is observed to contain structural information only to about 27°, corresponding to $d_{min} = 1.87$ Å. In addition, it is apparent that there are also diffraction lines from an ITQ-17 (i.e., BEC)[19] contaminant (Figure 1b). Attempts to index this pattern with Jade were fruitless, although a tetragonal unit cell with dimensions $a = 26.66$, $c = 13.38$ Å was favored but in an incorrect space group. Electron diffraction observations of the microcrystals were restricted initially by the extreme lath crystal thickness. After sectioning the sample in an ultramicrotome, more useful results were obtained. For example, it was possible to identify two possible orthogonal projections corresponding to [100] and [001] (Figure 2) in a tetragonal cell with dimensions $a = 26.10 \pm 0.16$, $c = 12.91 \pm 0.08$ Å. Patterns sampling tilts around the a^*-axis could be plotted on a two-dimensional grid, along with zonal patterns, to verify the assumption of a tetragonal cell. Systematic absences in the graphed three-dimensional reciprocal lattice followed the rules: hkl, $h + k + l = 2n + 1$; $hk0$, $h + k = 2n + 1$; $0kl$, $k + l = 2n + 1$; $00l$, $l = 2n + 1$, $0k0$, $k = 2n + 1$. Because the *hk*0 pattern in Figure 2a indicates that $|F(hk0)| = |F(kh0)|$, favoring a *p*4*mm* projection, there are several possible space groups,[20] viz *I*4/*mmm* (139), *I*-4*m*2 (119), *I*-42*m* (121), *I*4*mm* (107), and *I*422 (97), that also satisfy these extinction conditions. Only the first one is centrosymmetric. Because more than 90% of the zeolite crystal structures in the Atlas of Zeolite Framework Types[21] are centrosymmetric, most attention was paid to space group *I*4/*mmm*.

The contrasted distribution of intensity in the *hk*0 electron diffraction pattern (Figure 2) motivated an initial direct methods analysis with MICE, employing 41 *hk*0 and 17 0*kl* reflections. A Wilson plot based on these intensity data indicated an overall temperature factor, $B = 9.25$ Å^2, which was retained for the calculation of unitary structure factors. After using an origin-defining phase assignment $\phi(051) = 0°$, in the only reflection index parity class permitted for this

(9) Corma, A.; Jose Diaz, M.; Rey, F.; Strohmaier, K. G.; Dorset, D. L. World Patent WO 2007075382 A1, 2007.
(10) Grosse-Kunstleve, R. W.; McCusker, L. B.; Baerlocher, Ch. *J. Appl. Crystallogr.* **1999**, *32*, 536.
(11) Larsson, A. C.; von Dreele, R. B. *General Structure Analysis System, GSAS*; Los Alamos Laboratory: Los Alamos, NM, 1994.
(12) Baerlocher, Ch.; Hepp, A.; Meier, W. M. *Distance Least Squares Refinement Program, DLS-76*; ETH Zürich: Zürich, Switzerland1977.
(13) Zou, X. D.; Sukharev, Yu.; Hovmöller, S. *Ultramicroscopy* **1993**, *49*, 147.
(14) Zou, X. D.; Sukharev, Yu.; Hovmöller, S. *Ultramicroscopy* **1993**, *52*, 436.
(15) Hovmöller, S. *Ultramicroscopy* **1992**, *41*, 121.
(16) Gilmore, C. J.; Bricogne, G. *Methods Enzymol.* **1997**, *277*, 65.
(17) Gilmore, C. J.; Dong, W.; Dorset, D. L., *Acta Crystallogr.* **2008**, *A64*, 284, 295.
(18) Baerlocher, Ch.; McCusker, L. B.; Palatino, L. *Z. Kristallogr.* **2007**, *222*, 47.
(19) Corma, A.; Navarro, M. T.; Rey, F.; Rius, J.; Valencia, S. *Angew. Chem., Int. Ed.* **2001**, *40*, 2277.
(20) Hahn, Th. (ed.), *International Tables for Crystallography. Volume A. Space Group Symmetry*; Kluwer: Dordrecht, The Netherlands, 1995.
(21) Baerlocher, Ch.; McCusker, L. B.; Olson, D. H., *Atlas of Zeolite Framework Types*; Elsevier: Amsterdam, 2007.

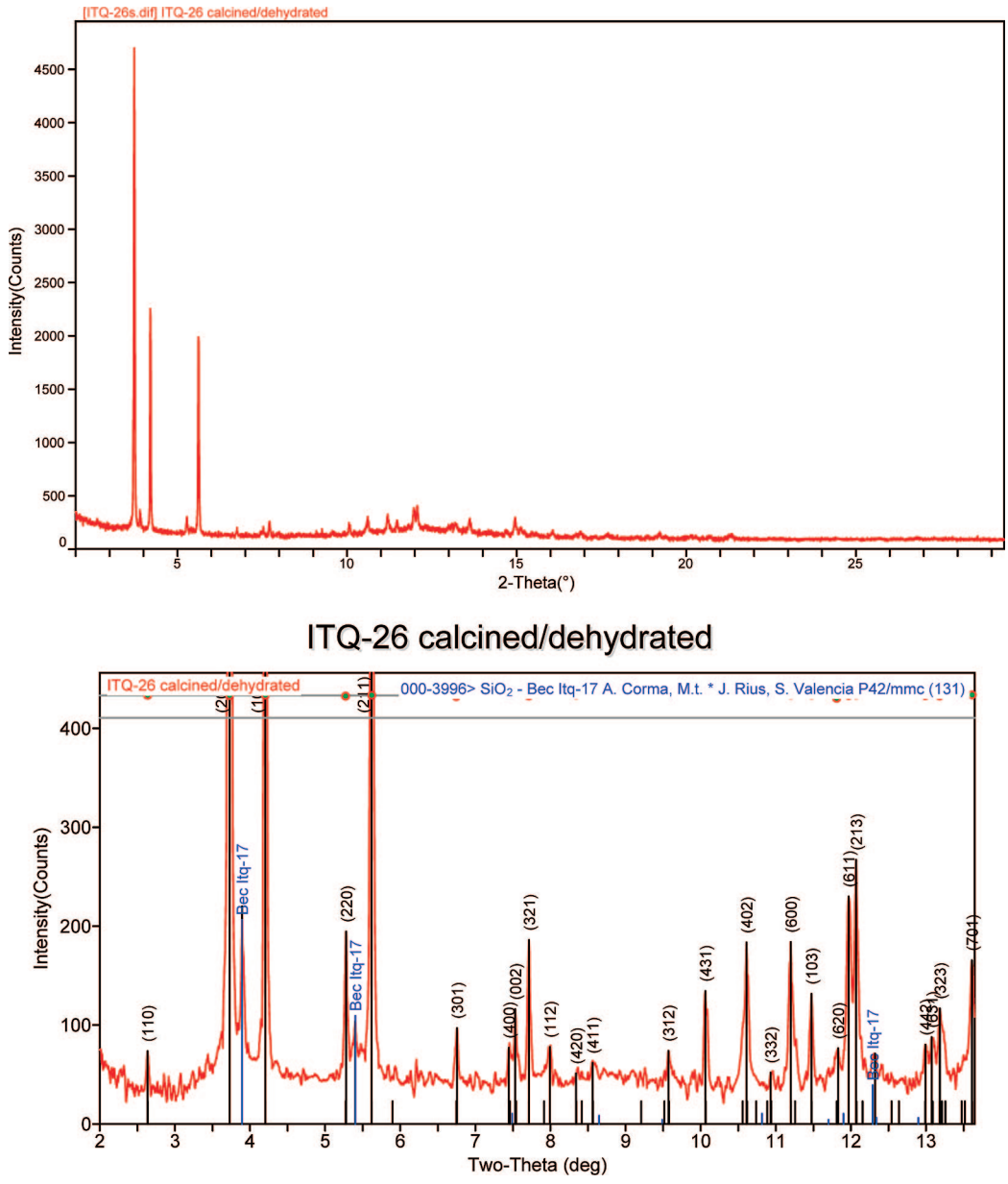

Figure 1. Synchrotron powder pattern from ITQ-26. Bottom shows lines from BEC impurity.

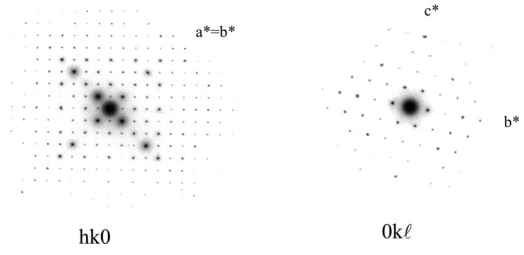

Figure 2. Electron diffraction patterns from ITQ-26.

space group,[22] a Nordström−Robinson error-correcting code was used to permute the phases of 16 other strong reflections.[23] A possible solution was observed at the sixth largest value of maximum likelihood (Figure 3) within the 256 generated trials, identified because of the presence of a 12-MR channel in keeping with earlier absorption measurements. Although some previous experience with direct phasing of electron diffraction data from zeolites[24,25] has demonstrated that such results should be treated with some caution, a promising [001] potential map was used as an additional reference point for direct methods trials with the synchrotron powder data.

A program for determining zeolite structures from powder diffraction data, FOCUS,[10] which utilizes a random crystallographic phase generator and employs a structure recognition algorithm for possible T-site connectivity in the analysis of trial maps, was applied to the experimental synchrotron intensity data that had been extracted via an equipartition method.[26] Only data extending to d = 2.28 Å were

(22) Rogers, D. In *Theory and Practice of Direct Methods in Crystallography*; Ladd, M. F. C., Palmer, R. A., Eds.; Plenum: New York, 1980; p 23.
(23) Gilmore, C. J.; Dong, W.; Bricogne, G. *Acta Crystallogr., Sect. A* **1999**, *55*, 70.
(24) Dorset, D. L. *Z. Kristallogr.* **2003**, *218*, 458–465.
(25) Dorset, D. L.; Gilmore, C. J.; Jorda, J. L.; Nicolopoulos, S. *Ultramicroscopy* **2007**, *107*, 462.
(26) LeBail, A.; Duroy, H.; Fourquet, J. L. *Mater. Res. Bull.* **1988**, *23*, 447.

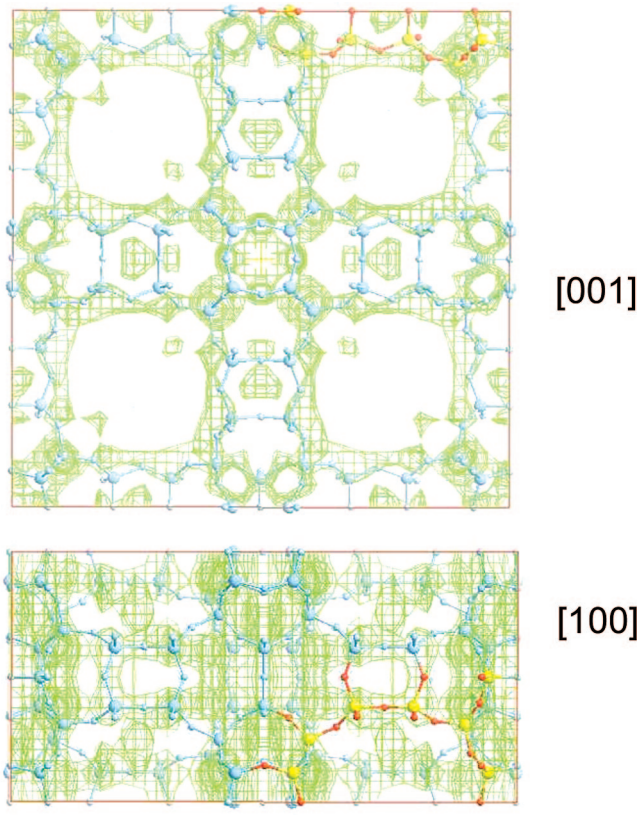

Figure 3. Direct phasing of electron diffraction data, ITQ-26, with MICE. Framework atom positions of actual structure are shown.

considered, and those from three narrow domains of 2θ containing diffraction peaks from the ITQ-17 contaminant were excluded. No models were generated if space groups other than *I*4/*mmm* were considered. An initial, promising model resembling the [001] projection in Figure 3, comprising 6 unique T-atoms, was not found to give reasonable T−O bonding geometry, also after exploring lower space group symmetries. Finally, after a long run of the FOCUS program with 500 000 trials, one model with 7 unique T-site positions was found among the 121 generated frameworks; this was found to conform to the observed powder diffraction data.

The 7 T-site framework is shown in Figure 4. After an initial DLS refinement, the framework atoms were refined by the Rietveld method against the experimental powder data (to $2\theta = 27°$, again excluding the ITQ-17 contaminant peaks), giving $R_{wp} = 0.0982$, $R(F^2) = 0.2396$. However, some T−O distances were somewhat large (e.g., 1.67 Å). This model was then readjusted energetically with the program DLS using one cycle to yield $R = 0.009120$. The new model had excellent bonding geometry. A further Rietveld refinement yields $R_{wp} = 0.0918$, $R(F^2) = 0.1924$, again with excellent bonding geometry. For the all-silica framework model, the refined unit-cell dimensions are $a = 26.7769(8)$, $c = 13.2505(5)$ Å. Average T−O bond distances are 1.618(4) Å, and bond angles are on average: OTO, 109.7 ± 2.2°; TOT, 152.4 ± 12.5°. Coordination sequences[27] and vertex symbols[28] are given in Table 1 for the unique T-sites. Aside from not including Ge sites, the major problem with this result is the need to impose a very low temperature factor on the Si-atom positions ($U = 0.001$ Å^2). (To simulate coexistence of Ge and Si atomic sites, occupancies for two Si positions were found to refine to 1.25 and 1.17, respectively).

The material, however, contains 20 mol % Ge, anticipated to be localized within the D4R units.[29] For example, refinement of T-site atomic occupancy finds that identified Si1 and Si2 positions increase in value corresponding to an

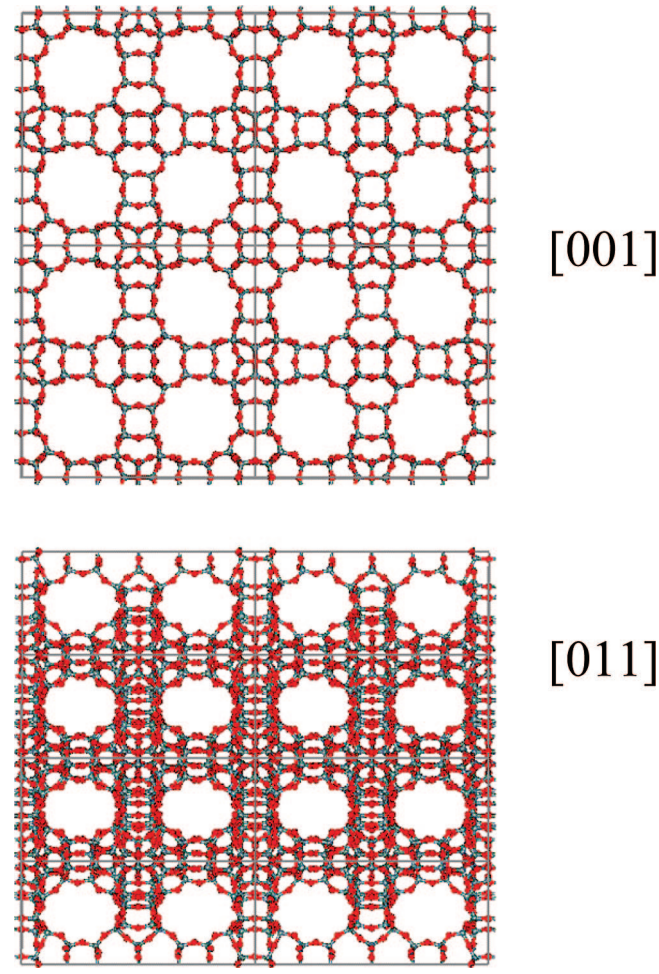

Figure 4. Framework model for ITQ-26 showing channels.

Table 1. Coordination Sequence and Vertex Symbol for ITQ-26 T-Sites

	T-site Coordination Sequence									
Si1	4	9	18	31	47	66	94	127	159	188
Si2	4	9	17	29	44	68	97	125	154	190
Si3	4	9	18	30	42	60	89	126	162	188
Si4	4	12	18	27	48	69	94	124	160	201
Si5	4	12	17	30	46	67	90	124	158	186
Si6	4	11	20	24	36	72	110	126	136	182
Si7	4	11	20	28	42	70	100	120	146	186

	T-Site Vertex Symbol					
Si1	4	5	4	6	4	12_3
Si2	4	5	4	6_2	4	12_3
Si3	4	6_2	4	6_2	4	12_4
Si4	5	6	5	6	6_2	12
Si5	5	5	5_2	12_3	6	6
Si6	4	5_2	6_2	6_2	6_2	6_2
Si7	4	5_2	5	6	5	6

(27) Meier, W. M.; Moeck, H. J. *J. Solid State Chem.* **1979**, *27*, 349.
(28) O'Keeffe, M.; Hyde, S. T. *Zeolites* **1997**, *19*, 370.

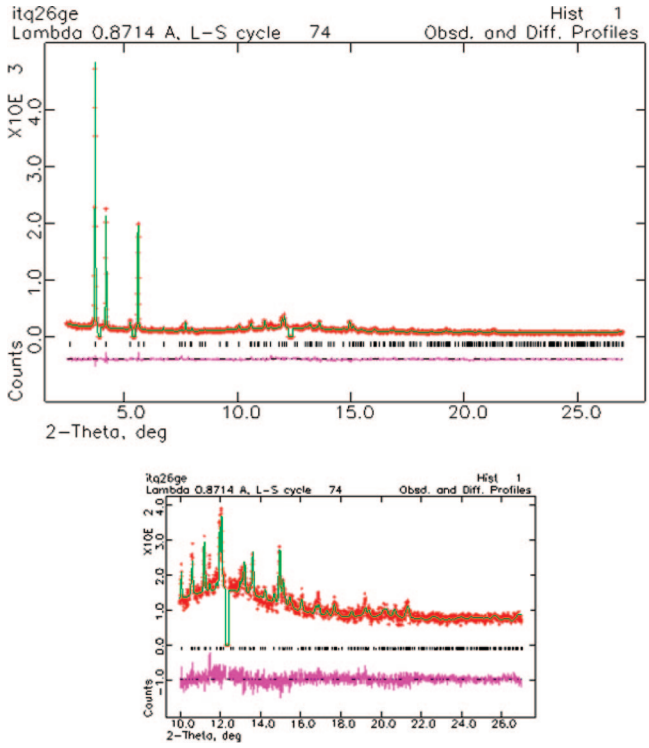

Figure 5. Rietveld refinement of germanosilicate model for ITQ-26.

anticipated increase of average Z-value (i.e., the sin $\theta/\lambda = 0$ value of the T-site X-ray scattering factors). A fractional model constructed with 0.34 Ge and 0.66 Si in positions within the D4R units yields, after Rietveld refinement (2θ range: 2.25 → 27°) (Figure 5): $R_{wp} = 0.0915$, $R(F^2) = 0.1799$, $R_p = 0.0702$, $\chi^2 = 1.141$, with the added advantage that all thermal parameters are now reasonable, e.g. $U = 0.025$ Å^2. A DLS refinement based on this model had refined to $R = 0.0043731$. Further Rietveld refinement on atomic coordinates did not result in a geometrically improved model, a criterion more important than mere lowering of crystallographic residuals.[30] The refined coordinate model that is nearly equivalent to the DLS refinement (i.e., giving the same R_{wp} and $R(F^2)$ figures of merit) model is given in Table 2. In this model, the average T−O distance is 1.62 ± 0.03 Å and average bond angles are OTO: 110.3 ± 5.2°, TOT: 147.3 ± 6.2°.

Discussion

As is expected for a material synthesized via Ge,[29] ITQ-26 (Figure 6) contains a number of double 4-ring (D4R) simple building units (Figure 7). However there are other more complex ones as well. For example, a component $6^2 5^4 4^2$ (msv) cage is a unit also found in MCM-68,[31] another multidimensional zeolite with 12-ring channels. However, this zeolite has a much higher framework density than ITQ-26, viz. 16.6 T/1000 Å^3 for MCM-68 vs 14.3 T/1000 Å^3 for ITQ-26, the latter close to the theoretical density for LTA.[32]

(29) Corma, A.; Diaz-Cabanas, M. J.; Martinez-Triguero, J.; Rey, F.; Rius, J. *Nature* **2002**, *418*, 514.
(30) McCusker, L. B.; Von Dreele, R. B.; Cox, D. E.; Louër, D.; Scardi, P. *J. Appl. Crystallogr.* **1999**, *32*, 36.
(31) Dorset, D. L.; Weston, S. C.; Dhingra, S. S. *J. Phys. Chem. B* **2006**, *110*, 2045.

Table 2. DLS Heteroatom Model for ITQ-26

atom	*x/a*	*y/b*	*z/c*	occ.
Ge1	0.0586(5)	0.3209(4)	0.1176(7)	0.32
Si2	0.0586(5)	0.3209(4)	0.1176(7)	0.68
Ge3	0.0584(4)	0.2043(4)	0.1179(6)	0.32
Si4	0.0584(4)	0.2043(4)	0.1179(6)	0.68
Ge5	0.0582(2)	0.0582(2)	0.3825(6)	0.32
Si6	0.0582(2)	0.0582(2)	0.3825(6)	0.68
Si7	0.1050(3)	0.1050(3)	0.1891(6)	1.00
Si8	0.0884(3)	0.4116(3)	0.25	1.00
Si9	0.0574(2)	0.0574(2)	0.0	1.00
Si10	0.0	0.4427(2)	0.3837(4)	1.00
O11	0.0629(2)	0.3410(9)	0.0	1.00
O12	0.0	0.3194(1)	0.1550(3)	1.00
O13	0.0791(7)	0.2625(3)	0.1238(2)	1.00
O14	0.0876(4)	0.3568(3)	0.1983(1)	1.00
O15	0.0948(4)	0.1645(3)	0.1785(1)	1.00
O16	0.0571(2)	0.1849(1)	0.0	1.00
O17	0.0	0.2020(1)	0.1599(2)	1.00
O18	0.0726(7)	0.0726(7)	0.5	1.00
O19	0.0	0.0718(5)	0.3565(2)	1.00
O20	0.0924(2)	0.0924(2)	0.3049(6)	1.00
O21	0.0755(3)	0.0755(3)	0.1059(4)	1.00
O22	0.0845(4)	0.4517(2)	0.1624(5)	1.00
O23	0.0	0.0711(6)	0.0	1.00
O24	0.0	0.5	0.3529(4)	1.00
O25	0.0	0.4290(5)	0.5	1.00

Two other zeolites, BEC[19] and ISV,[33] 3-dimensional frameworks with 12-rings, have similarly low framework densities around 15.0 T/1000 Å^3, and possess the same arrangement of the msv cages. Essentially, the structure of ITQ-26 (Figure 6) combines features of BEC[19] and ITQ-21[29] frameworks as shown in Figure 7. The BEC part again includes the stacking of four 5-membered rings with D4R units along one set of 4-fold axes, cited above. The other 4-fold axes contain stacked $[4^6 6^{12}]$ cages (similar to ITQ-21) interspersed with D4R units. Although the $[4^6 6^{12}]$ cage is disordered in the cubic ITQ-21 crystal structure,[29] involving a random orientation of a central 4-MR segment among three possible positions, there is no evidence for such disorder in ITQ-26. (For example, there is no salient continuous diffuse scatter or streaking in the *hk*0 and 0*kl* electron diffraction patterns

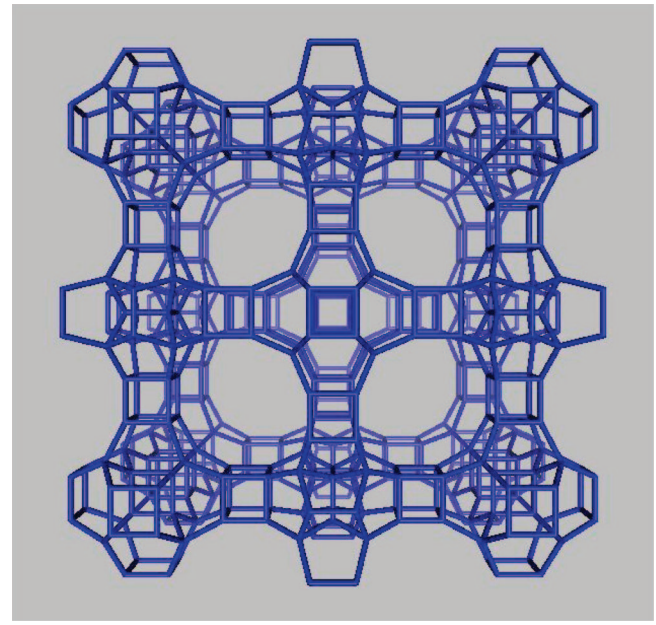

Figure 6. Perspective view of ITQ-26 framework.

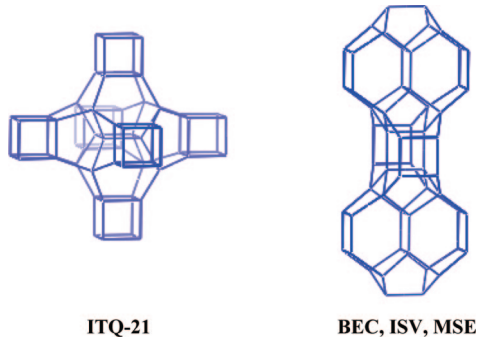

Figure 7. Secondary building units for ITQ-26. The ITQ-21 unit with D4Rs, left. The msv cages arranged in way similar to BEC, ISV, and MSE structures, right.

(Figure 2).) From periodic bond chain models for crystal growth,[34,35] the lack of disorder within the $[4^6 6^{12}]$ cage is consistent with the tetragonal crystal structure of ITQ-26. The lathlike crystal habit with square cross-section grows most rapidly along the [001] direction, consistent with a directional stacking of the cage where the 4-MR plane is maintained perpendicular to [001]. Less rapid growth is found laterally in the 4-fold projection and this growth, moreover, is more isotropic, also consistent with the projected 4-fold symmetry of the embedded small ring segment.

ITQ-27[5] crystallizes in a unit cell dimensionally similar to ITQ-26 with 12-ring channels with D4R simple building units and a much different connectivity to construct a denser framework. However this orthorhombic material is only two-dimensional with one oblique channel whereas the tetragonal symmetry of ITQ-26 gives a three-dimensional array including two oblique channels oriented along ⟨011⟩. In projection, the structure of ITQ-26 also resembles somewhat that of OSI.[36] The latter is much denser and has a quite different connectivity along a tetragonal *c*-axis, although there is a simple columnar stacking of $6^4 4^2$ units (part of the ordered $[4^6 6^{12}]$ cages, considering the 4-MR insert) without interspersed D4R.

Germanium-containing zeolites are known to be stable in air in the as-synthesized form. Once calcined and the structure-directing agent removed, the framework germanium is susceptible to hydration in ambient air, which ultimately results in loss of crystallinity. If the calcined Ge-containing zeolite is prevented from rehydration either by handling in a dry atmosphere or keeping the sample above a temperature at which water absorption is minimized, the framework structure can be preserved. Because care was taken to handle calcined ITQ-26 in an inert atmosphere before measuring nitrogen absorption (Figure 8), the relatively low surface area (257 m^2/g) and pore volume (0.12 cm^3/g) are due to the apparent loss of crystallinity during the calcination step and not by subsequent rehydration. This reflects the lower stability of germanium as a tetrahedral framework atom compared to silicon. The loss of crystallinity is reflected in

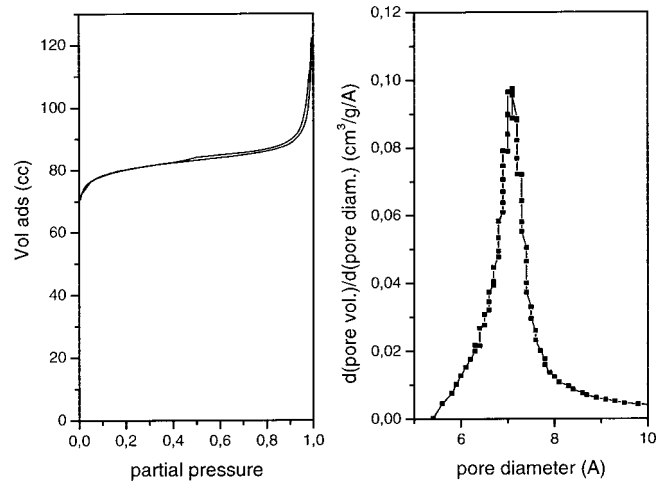

Figure 8. Nitrogen absorption isotherm (left) and argon pore size distribution (right).

the broad amorphous peak centered at 4.16 Å in the X-ray diffraction pattern of calcined ITQ-26 and in the low value of the measured pore volume. Three-dimensional, low-framework-density zeolites, such as faujasite and chabazite, typically have pore volumes greater than 0.25 cm^3/g. Although a $Ge_{0.2}Si_{0.8}O_2$ composition is 15% heavier than a pure SiO_2 composition, the ITQ-26 pore volume of 0.12 cm^3/g still represents a loss of least 50% of its expected pore volume.

The 12-member ring channels of ITQ-26 down the [001] direction are straight and have a diameter of 7.05 Å as determined from the refined atomic positions of the oxygen atoms using an oxygen diameter of 2.7 Å. The other two 12-member ring channels are sinusoidal and run along the [011] directions. These are slightly elliptical in shape and have size of 7.02 × 7.30 $Å^2$, although a molecule must pass through the 7.05 Å pore to get to the next 7.02 × 7.30 $Å^2$ pore. The pore sizes of the 12-member pores are in agreement with the pore size of 7.1 Å determined from argon absorption (Figure 8) using the Horváth−Kawazoe[37] equation.

Because of poor data quality, this was a difficult structure to determine from synchrotron data. At the 2.28 Å resolution used to seek a solution via FOCUS,[10] adjacent T, O atomic positions would be distinguishable if the Rayleigh limit were $0.61 d_{min}$, but less so if this limit were actually $0.715 d_{min}$.[38] The former limit would correspond to the interpretation of 2D electron density maps and the latter to 3D maps. However, Stenkamp and Jensen[38] pointed out that the actual resolution may be far worse, $0.917 d_{min}$, for experimental maps calculated from observed diffraction amplitudes.

It is interesting to note how well the ab initio electron diffraction analysis fared with the patterns obtained from sectioned samples. Even though the data obviously are modified by multiple scattering effects, it is astonishing how close the density maxima in Figure 3 are to actual T-sites. Also in the [100] projection where there were fewer data, many of the T-sites lie within density maxima. The overall rms phase error is 73° for all reflections and 66° for those

(32) Reed, T. B.; Breck, D. W. *J. Am. Chem. Soc.* **1956**, *78*, 5972.
(33) Villaescusa, L. A.; Barrett, P. A.; Camblor, M. A. *Angew. Chem., Int. Ed.* **1999**, *38*, 1997.
(34) Hartman, P.; Perdok, W. G. *Acta Crystallogr.* **1955**, *8*, 49.
(35) Hartman, P.; Perdok, W. G. *Acta Crystallogr.* **1955**, *8*, 521.
(36) Akporiaye, D. E.; Fellvåg, H.; Halvorsen, E. N.; Haug, T.; Karlsson, A.; Lillerud, K. P. *Chem Commun.* **1990**, 1553–1554.
(37) Horvath, G.; Kawazoe, K. *J. Chem. Eng. Jpn.* **1983**, *16*, 470.
(38) Stenkamp, R. E.; Jensen, L. H. *Acta Crystallogr., Sect. A* **1984**, *40*, 251.

where $|F_{obs}| > 2.0$ (relative scale). Although the structure analysis of SSZ-48 from electron diffraction data[39] also relied on intensity data from sectioned samples, this is the first success realized in this laboratory with such a sample.

It is quite fortunate that a useful structural model was found by MICE from electron diffraction data within the first few phase solutions ranked according to maximum likelihood.[16] Recent experience[17,25] reveals that multiple scattering perturbations, even after data are collected via a precession device for the electron microscope on imaging plates, cause the most informative phase solutions to be placed much lower in such a listing sorted by this FOM. If the zeolite density histogram is employed to rerank these phase solutions, another good map is found where the fit of the actual zeolite framework structure to the potential map is even closer than found before.

Although procedures for phasing electron diffraction amplitudes from zeolites require further development, the outlook for solving unknown structures is not hopeless. Clearly, much of the success of an ab initio determination depends on the quality of the recorded intensity data. In other words, how close are these data to the Fourier transform of the actual Patterson function? Although precession techniques and nonfilm methods for recording diffraction intensity are useful,[25] the decisive factor is the quality of the crystalline preparation itself. One needs crystals that are adequately thin and projections onto the most informative views of the crystal structure (e.g., channel openings).

(39) Wagner, P.; Terasaki, O.; Ritsch, S.; Nery, J. G.; Zones, S. I.; Davis, M. E.; Hiraga, K. *J. Phys. Chem. B* **1999**, *103*, 8245.

Conclusion

ITQ-26 was been synthesized via the fluoride route using 1,3-bis-(triethylphosphoniummethyl)-benzene as the structure-directing agent. The framework was determined from both powder X-ray diffraction and electron diffraction data, with the aid of the FOCUS and MICE algorithms, repectively. The structure of calcined/dehydrated form was subsequently refined from synchrotron powder diffraction data using Rietveld methods in space group *I4/mmm*, where $a = 26.7792(8)$, $c = 13.2510(6)$ Å. ITQ-26 is a new 3-dimensional, 12-ring pore zeolite with structural building units similar to those in the BEC, ISV, and ITQ-21 frameworks.

CM801126T